Journal of Neuro-Oncology **9**: 17–28, 1990.

Laboratory Investigation

Relationship between of blood flow, glucose metabolism, protein synthesis, glucose and ATP content in experimentally-induced glioma (RG1 2.2) of rat brain

G. Mies, W. Paschen, G. Ebhardt[1] and K.-A. Hossmann
Max-Planck-Institut für neurologische Forschung Abteilung für experimentelle Neurologie and
[1] Institut für Pathologie, Sektion Neuropathologie der Krankenanstalten Köln,
Merheim Ostmerheimer Str. 200, D-5000 Köln 91, FRG

Key words: brain tumor, triple tracer autoradiography, blood flow, glucose metabolism, protein synthesis, energy state, thresholds

Summary

In experimental RG1 2.2 glioma of rat brain, local blood flow, glucose utilization, protein synthesis, glucose and ATP content were measured by means of triple tracer autoradiography and bioluminescence technique, respectively, to determine hemodynamic and metabolic thresholds for local tumor energy failure. Perfusion thresholds were estimated at tumor blood flow values of 69.0 ± 0.1 ml/100 g/min (estimate ± standard error) and of 69 ± 7.1 ml/100 g/min for the beginning of the decline in regional ATP and glucose content, respectively. Metabolic thresholds were derived at tumor glucose utilization values of 70.6 ± 8.3 μmol/100 g/min for reduced protein synthesis, of 55.0 ± 0.2 μmol/100 g/min for the decrease in glucose content, and 34.7 ± 4.7 μmol/100 g/min for decline in ATP content. Our results suggest that blood flow limits glucose supply to tumor tissue at much higher flow rates than in normal brain which, in turn, is associated with a decrease in tumor glucose utilization. A reduction and not an increase in tumor glucose availability could be a more appropriate strategy for the induction of energy failure in tumors.

Introduction

The efficiency of non-surgical procedures for the treatment of brain tumors depends on a selective sensitivity of the tumor tissue to therapeutic interventions which are not effective in normal brain tissue. The development of therapeutic strategies, therefore, must be based on inherent differences between the metabolic-hemodynamic properties of brain and tumor tissue. One of these characteristic differences is the remarkable tendency of brain tumors to exhibit spontaneous necrosis. It is reasonable to assume that enhancement of processes involved in the development of spontaneous tumor necrosis could contribute substantially to the efficacy of therapeutic interference such as X-ray irradiation, hyperthermia, or chemotherapy.

The mechanisms responsible for the spontaneous onset of tumor necrosis are still poorly understood. Factors contributing presumably include a disturbed relationship between blood flow and the substrate demands of tumor parenchyma possibly related to impairment of tumor angiogenesis, accumulation of metabolites, and persistence of tumor tissue acidosis. The respective roles of hemodynamic and metabolic factors contributing to spontaneous tumor necrosis, however, have not been established. In particular, the perfusion thresholds which have to be reached to achieve such a therapeutic effect are not yet known.

In order to determine these thresholds, three methodological requirements are necessary: first, a reproducible animal tumor model which can be investigated repeatedly at the same stage of tumor growth; second, multiparametric regional methods for the simultaneous measurement of blood flow, and metabolism, and third, an approach to data analysis which allows the objective estimation of threshold-dependent relationships between parameters of interest.

In the past, a variety of experimental tumor models have been established. Tumors have been induced by transplacental, systemic or local application of chemical carcinogens, by transplantation, by intracarotid or intracerebral injection of suspended neoplastic cells. Examples are the ethylnitrosourea-induced oligodendroglioma or mixed glioma [1], avian sarcoma virus induced anaplastic or polymorphic astrocytoma [2], metastatic Walker-255 carcinoma [3], or the implantation of cloned tumor cells such as RG1 2.2 [4] or RT9 glioma [5]. For the present study we chose the RG1 2.2 glioma because intracerebral growth of this tumor exhibits a high degree of reproducibility after stereotaxic inoculation.

With the introduction of multiparametric imaging techniques [6], it has become possible to analyze in detail the local blood flow and metabolic parameters of these tumors. Quantitative autoradiographic techniques for the study of cerebral blood flow [7], local cerebral glucose utilization [8] and local cerebral protein synthesis [9] can be combined by the appropriate choice of radioactive labels for simultaneous measurement in the same animal and the same brain section [10, 11]. In addition, biochemical substrates such as ATP and glucose can be imaged using the principle of substrate-induced bioluminescence [12–14]. For threshold analysis, two-dimensional data plots can be submitted to piecewise linear regression which allows the estimation of a breakpoint parameter value [15] at the interception of two linear regression lines. This breakpoint parameter value represents the threshold value for the relationship between the independent and dependent variables.

In the present study these techniques were applied for the investigation of the relationship between perfusion and metabolism of experimentally-induced rat gliomas (RG1 2.2) in order to determine the hemodynamic and metabolic thresholds for local energy failure possibly related to spontaneous necrosis.

Material and methods

Experimental groups

Experiments were carried out in seven female BD IX rats weighing 200–250 grams. Two animals were healthy controls and five animals had been implanted with the rat glioma clone RG1 2.2 three weeks before measurements.

Induction of brain tumors

Rats were anesthetized with pentobarbital (50 mg/kg ip.) and the heads were fixated in a stereotaxic frame. A burr hole of about 1 mm in diameter was drilled over the right hemisphere at coordinates of 0.5 mm posterior and 2.5 mm lateral to bregma under sterile conditions. A micro-volume syringe containing the suspended tumor cells (20000 cells per 10 μl) was attached to a micro-manipulator, and the tip of the needle was inserted through the burr hole 4.8 mm below the surface of the dura. The tumor cell suspension was injected slowly over 15 seconds and the injection needle was left in place for one minute to avoid efflux of the tumor cell suspension through the needle tract. After transplantation, the skin wound was sutured and the animals were returned to their cages.

During the following three weeks rats were regularly investigated for neurological symptoms but did not exhibit any abnormalities. In particular, no symptoms of drowsiness or lethargic behavior were detected indicating the absence of intracranial hypertension during the observation period.

Animal preparation for tracer application

Control and tumor-bearing animals (three weeks

after tumor cell transplantation) were anesthetized with pentobarbital (50 mg/kg ip.). Polyvinyl catheters were inserted into both femoral arteries and veins for recording of systemic blood pressure, sampling of arterial blood, and intravenous injection of drugs and labeled tracers. After tracheotomy, rats were immobilized with d-tubocurarine chloride (1.5 mg/kg iv.) and mechanically ventilated using a rodent respirator. Minute ventilation was adjusted to yield an arterial pCO_2 of about 40 mmHg. Body temperature was kept constant at 37° C with a feed-back controlled infrared heating lamp. Prior to tracer application arterial blood gas analysis was performed.

Autoradiographic determination of blood flow, glucose utilization and protein synthesis

In all rats, local blood flow, glucose consumption and protein synthesis were assessed by using triple tracer autoradiography [11]. Rats received an intravenous bolus of ^{14}C-2-deoxyglucose (^{14}C-DG: 100 μCi/kg; specific activity 300–350 mCi/mmol; NEN, Dreieich, FRG) and metabolic rate for glucose in brain (CMRglc) and tumor (TMRglc) was measured as described elsewhere [8]. 15 min later, five tritiated amino acids (^{3}H-AS; 500 μCi/kg: phenylalanine (100 Ci/mmol), tyrosine (70 Ci/mmol), isoleucine (80 Ci/mmol), leucine (120 Ci/mmol), methionine (70 Ci/mmol); NEN, Dreieich, FRG) were injected for measurement of incorporation of amino acids into brain (CPS) and tumor proteins (TPS). 45 min after application of ^{14}C-DG, cerebral blood flow was measured with ^{131}I-iodoantipyrine (^{131}I-IAP: 1 mC/kg; specific activity 7.45 mCi/mg; NEN, Dreieich, FRG). ^{131}I-IAP was infused at a constant rate for 1 min and arterial blood samples were collected repeatedly. After 55 sec in situ freezing of brains with liquid nitrogen was commenced. Arterial ^{131}I-IAP blood and ^{14}C-DG plasma radioactivities were determined in a gamma counter (Biogamma II, Beckman, Fullerton, CA, USA) and a scintillation counter (L 7000, Beckman, Fullerton, CA, USA), respectively. Arterial plasma glucose concentration was measured using an automated assay based on the glucose oxidase reaction (Glucose Analyzer 2, Beckman, Fullerton, CA, USA).

After termination of in situ freezing, brains were immediately removed and placed in a cold box at − 20° C and cut into 20 μm thick coronal cryostat sections at − 20° C (Cryocut, SLEE, Mainz, FRG). Adjacent 20 μm tissue slices were mounted on cover slips at − 20° C and kept at − 80° C for subsequent bioluminescence determination of regional tissue ATP and glucose content as described below. Autoradiographic differentiation of ^{131}I,^{14}C and ^{3}H in the same brain section was achieved as described previously [11]. ^{131}I-IAP autoradiography was performed together with ^{131}I-brain standard sections of different isotope concentrations exposed immediately to Kodak NMB film for 24 hours. After complete decay of ^{131}I, ^{14}C-autoradiography of brain sections and calibrated ^{14}C standards was carried out by exposure to Kodak NMB film for two weeks to obtain images in which blackening represents total ^{14}C-tissue radioactivity. Following treatment of the brain slices with 10% trichloroacetic acid, 70% ethanol, 2% polyvinylpyrrolidone, and 0.1% Nonidet-NP-40 remaining ^{14}C tissue activity was assessed by re-exposure to Kodak NMB film for two weeks. Then incubated sections were autoradiographed with LKB Ultrofilm for two weeks. In these images, blackening of the film results from the incorporation of ^{3}H-labeled amino acids into cerebral proteins and from residual ^{14}C tissue radioactivity.

Densitometry of autoradiograms was carried out with a microdensitometer (Scandig 3, Joyce Loebl, Gateshead, UK) which was driven by a laboratory computer (PDP 11/24, Digital Equipment, Maynard, MA, USA). Digitized images were processed with an image processor (ID 2200, DeAnza, St. Clara, CA, USA) using a modified version of the original software [16]. Quantitative determination of local ^{131}I and ^{14}C tissue activities was performed by converting local optical density values to isotope radioactivity using a calibration curve of the relationship between optical density and the concentrations of the isotope standards. ^{3}H-induced radioactivity determined in LKB film autoradiograms was corrected for residual ^{14}C radioactivity by digital subtraction [11]. Regional evaluation of cere-

bral blood flow and glucose utilization was performed by outlining brain areas in the regions of interest. Non-invaded brain structures of the tumor-housing hemisphere were considered as adjacent to the glioma, brain regions of the tumor-opposite hemisphere as remote from the tumor mass. Parametric evaluation of the various tumor parameters was achieved in aligned images scanned at 75 μm intervals by chosing regions of interest (ROI) of 5 × 5 pixels. The ATP bioluminescence images were used as guide images to visualize tumor energy depletion and thus of tumor energy failure. The horizontal projection through such areas of the tumor was then used to choose viable tumor ROIs' in images representing the other parameters. Local blood flow in brain (CBF) and tumor tissue (TBF) was calculated according to Sakurada *et al.* (1978). A tissue/blood partition coefficient λ of 0.8 was used for both normal and pathological tissue. Local metabolic rates of glucose in brain (CMRglc) and tumor tissue (TMRglc) were calculated by the operational equation of Sokoloff *et al.* (1977) using the rate and the lumped constants of awake albino rats. Cerebral protein synthesis (CPS), so far, cannot be determined quantitatively because the integrated specific activity of aminoacyl-tRNA differs from that of plasma [49] by a factor of approximately 0.6. Local ^{3}H-labeled tumor protein activity, therefore, was expressed as a percentage of that in the contralateral cortex. This allows a qualitative estimation of tumor proteins synthesis (TPS) relative to protein synthesis in non-invaded brain tissue as a reflection of the capacity of the protein synthesizing machinery of tumor tissue.

Following triple autoradiography, brain sections were stained with hematoxylin-eosin (HE) and examined for sinusoidal tumor vessels and for focal hemorrhages.

Measurement of regional ATP and glucose content

In alternate brain sections the regional ATP [12, 14] and glucose content [13] was imaged by substrate-induced bioluminescence. Brain slices were freeze-dried and covered with 60 μm thick sections of frozen solution containing all enzymes, coenzymes and cofactors necessary for the substrate-specific bioluminescence reaction. The light emission occurring immediately after thawing of the tissue/enzyme bilayer was recorded on photographic film (Agfa Pan, 200 or 400 ASA). Optical densities in these images was digitized with the image processing system as described above. Extinction values in bioluminescence images have been shown to correlate linearly with substrate concentration [17]. Local tumor ATP and glucose concentrations, therefore, were expressed as a percentage of the optical density measurement from the opposite hemisphere.

Data analysis

Tumor regions of interest of two parameters were submitted to piecewise linear regression analysis. Coefficients a, b and c, and the breakpoint parameter B were estimated by minimizing for least squares according to Neter *et al.* (1985)

$$Y = a + b \star X + c \star (X - B) \star R$$

Table 1. Physiological parameters

	pH_a	P_aCO_2 (mmHg)	P_aO_2 (mmHg)	MABP (mmHg)	Plasma glucose (μmol/ml)
Controls	7.422	39.8	170.3	137.5	7.2
(n = 2)	± 0.03	± 2.0	± 18.7	± 3.54	± 0.4
Tumor rats	7.399	41.4	161.3	113.2	5.3
(n = 5)	± 0.03	± 1.2	± 52.9	± 18.0	± 0.5

All values are expressed as means ± standard deviation.

where R is the constraint $X > B$ for $c \star (X - B)$. The estimate of B provides the numerical value at which the linear regression slopes of independent versus dependent variables differ. Systemic variables were compared in control and experimental animals by the nonparametric Mann-Whitney U-test. The relationship between blood flow and glucose utilization in non-tumorous tissue was examined by linear regression and correlation analysis [18]. A p-value < 0.05 was regarded as statistically significant.

Results

Physiological variables

Table 1 summarizes the mean values of systemic parameters measured in control and tumor rats prior to tracer application. No significant differences were noted.

Morphological observations

Following inoculation of RG1 2.2 glioma cells, spheric tumors developed in the right caudatus-putamen of all experimental animals. In three of five rats, the tumor caused a midline shift. Peritumoral white matter was swollen due to the spread of vasogenic edema fluid from the tumor. In one animal, the right lateral ventricle was enlarged because of partial occlusion of the interventricular foramen. Brain tumors induced by inoculation of RG1 2.2 cells have been classified histologically as anaplastic oligodendroglioma [19, 20]. Tumor cells were isomorphic and exhibited chromatin rich nuclei surrounded by pale cytoplasma. The density of tumor cells varied only moderately. Most frequently a loose network of cells was observed in the solid parts of the tumor. Palisade-shaped strings of tumor cells were located irregularly around cysts and necrotic areas and tended to be more eosinophilic. Cysts were filled with plasma-like fluid, traces of debris or bridges of viable tumor tissue. Confluent tumor hemorrhages were observed occupying an area of 0.5 to 1.5 mm^2.

Blood flow, glucose utilization and energy state

Table 2 summarizes mean values of regional cerebral blood flow (CBF) and cerebral glucose utilization (CMRglc). In control rats regional blood flow ranged between 50 and 109 ml/100 g/min. In tumor bearing rats, blood flow in ipsilateral cortex, and the opposite caudatus-putamen and thalamus decreased by about 30%, and in the ipsi- and contralateral hippocampus by 19%.

In control rats, regional mean glucose utilization values ranged between 33 and 57 μmol/100 g/min (Table 2). In tumor rats glucose utilization was

Table 2. Cerebral blood flow and glucose utilization in control and tumor rats

	Blood flow (ml/100 g/min)			Glucose utilization (μmol/100 g/min)		
	controls (n = 2)	tumor rats (n = 5)		controls (n = 2)	tumor rats (n = 5)	
		ipsil.	contral.		ipsil.	contral.
Parietal cortex	109 ± 13	70 ± 19	91 ± 25	57 ± 2	38 ± 10	38 ± 12
Temporal cortex	99 ± 8	78 ± 18	85 ± 16	53 ± 3	36 ± 4	40 ± 13
Caudatus-putamen	105 ± 12	–	67 ± 9	55 ± 4	–	39 ± 13
Thalamus	109 ± 9	79 ± 8	71 ± 10	50 ± 3	37 ± 7	38 ± 6
Hippocampus	67 ± 4	54 ± 10	55 ± 9	42 ± 3	34 ± 6	35 ± 6
White matter	50 ± 5	39 ± 2	49 ± 9	33 ± 4	21 ± 3	25 ± 5
Tumor tissue	–	73 ± 32	–	–	87 ± 48	–

All values are expressed as means ± standard deviation. n is the number of animals.

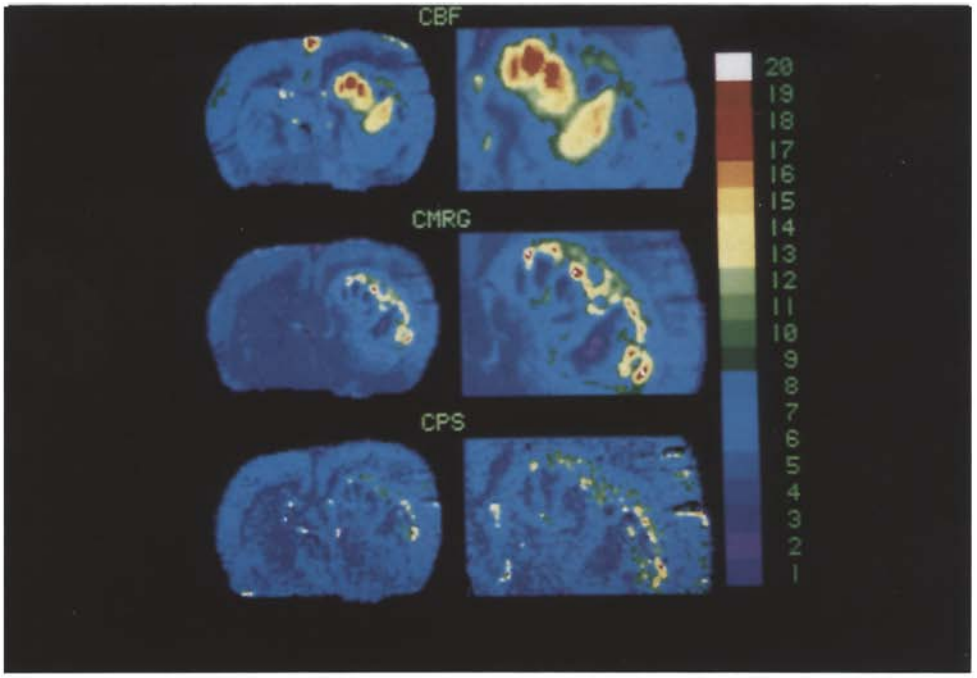

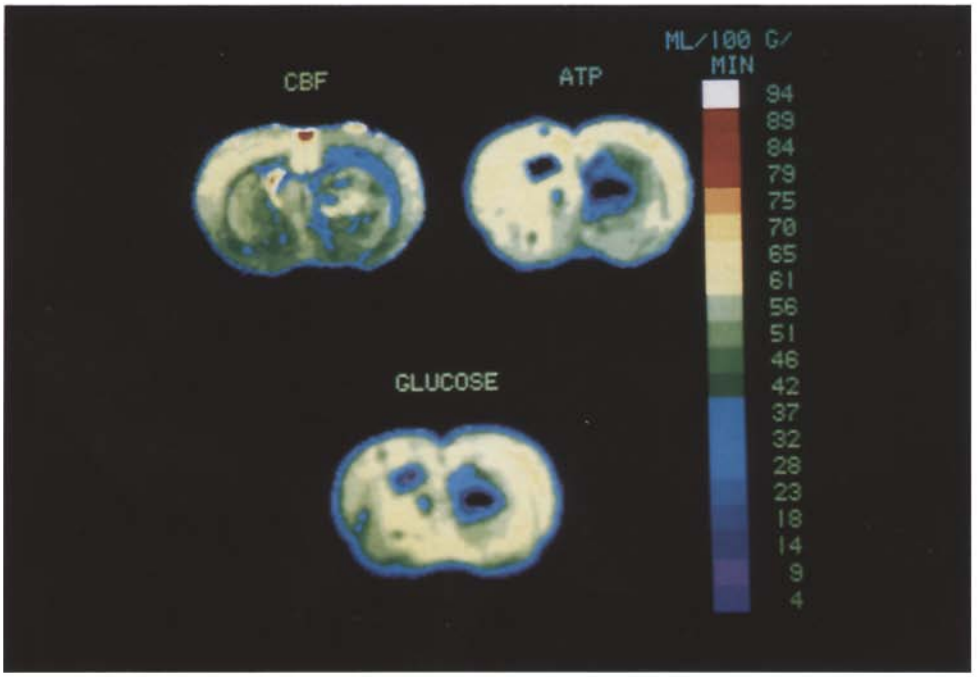

Fig. 1 A. Color-coded triple-tracer autoradiograms representing cerebral blood flow (CBF), glucose utilization (CMRG), and protein synthesis (CPS) from an identical brain section. The tumor tissue is delineated best in the CMRG-autoradiogram occupying the area of the striatum. Hot spots in CBF autoradiograms are related to tumor hemorrhages. Note that tumor blood flow (TBF) is not increased in areas in which glycolytic activity is drastically stimulated. Local tumor protein labeling expressed as percentage ^{3}H-radioactivity of contralateral cortex correlates with increments in tumor glucose utilization but is suppressed in discrete tumor areas when local glucose utilization exceeds a metabolic rate of 70 μmol/100 g/min (for quantification of blood flow and glucose utilization see Table 3).
Fig. 1 B. Color-coded images of blood flow (CBF), regional ATP and glucose content. A reduction in local tumor glucose and ATP content begins at flow rates below 70 ml/100 g/min. With declining tumor blood flow, energy state deteriorates further towards centrally located parts of the tumor mass. Note hermorrhage of tumor tissue as indicated by the high [^{131}I]-radioactivity but depletion of ATP and glucose content.

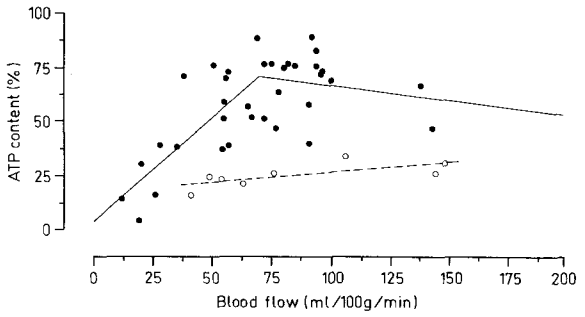

Fig. 2. Relationship between local tumor blood flow (TBF) and ATP content (% optical density of contralateral hemisphere). A flow threshold of 69.0 ± 0.04 ml/100 g/min (estimate ± standard error of the estimate) was determined by piecewise linear regression analysis below which flow rate tumor ATP content began to deteriorate (n = 4; closed circles). In one tumor-bearing rat which revealed the lowest tumor ATP content (21.8 ± 10.4% of that of the opposite hemisphere), the local energy state remained severely impaired despite TBF values ranging from 37 to 150 ml/100 g/min (open circles; $y = 17.1 + 0.0095 \star x$, $r = 0.717$).

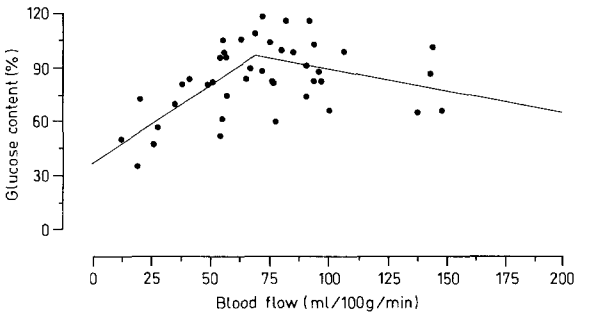

Fig. 3. Relationship between local tumor blood flow (TBF) and glucose content (% optical density of contralateral hemisphere). Piecewise linear regression analysis revealed a TBF threshold of 69.0 ± 7.1 (estimate ± standard error of the estimate) below which local tumor glucose content gradually declined with decreasing tumor perfusion.

suppressed by more than 30% in ipsilateral parietal and temporal cortex and contralateral parietal cortex. Similar decreases were observed in the caudatus-putamen, thalamus, and hippocampus.

Regional glucose and ATP content in the tumorous hemisphere were expressed as a percent of levels in the opposite hemisphere. In cortex, glucose content amounted to 100.9 ± 4.2% and ATP to 91.6 ± 13.2% (mean ± SD). These differences between hemispheres were not statistically significant.

In the tumor, local blood flow (TBF) ranged from 12 to 148 (mean ± SD: 73 ± 31 ml/100 g/min) and glucose utilization (TMRglc) from 9 to 211 (mean ± SD: 87 ± 48 μmol/100 g/min) (Fig. 1A). Local tumor ATP content was also more heterogeneous and amounted to 4–89% of that in the opposite hemisphere (mean ± SD: 51.9 ± 23.6%). Tumor glucose content varied between 35 to 118% (mean ± SD: 83.4 ± 21.0%) (Fig. 1B).

Correlation between tumor perfusion, metabolism, and energy state

– Local relationship between TBF and tumor ATP and glucose.

In one tumor, local ATP content was only 21.8 ± 10.4% (mean ± SD) of that in the opposite hemisphere although ATP content in the overlying cortex was 95%. In the other four tumors, average ATP levels ranged from 40.1 ± 8.5 to 70.2 ± 12.9% (mean ± SD) of levels in the opposite hemisphere, respectively. In the four tumors (Fig. 2; closed circles), local ATP content declined below a perfusion threshold of 69.0 ± 0.04 ml/100 g/min (breakpoint value). Below 12 ml/100 g/min, tumor ATP levels was less than 9%. In the fifth animal,

Table 3. Codes for color bars of Fig. 1A

	Codes									
	2	4	6	8	10	12	14	16	18	20
CBF (ml/100 g/min)	12	22	34	50	66	86	110	138	182	234
CMRglc (μmol/100 g/min)	3	10	25	42	65	90	119	156	196	243

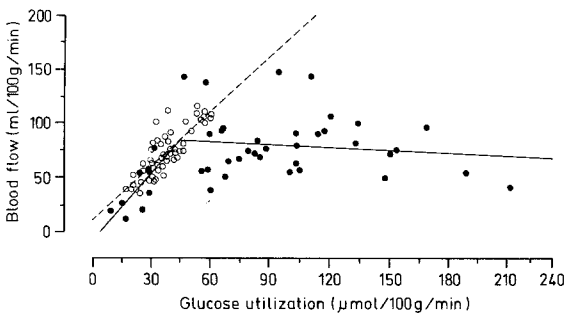

Fig. 4. Relationship between local glucose utilization in brain (CMRglc) and tumor tissue (TMRglc), and blood flow in brain (CBF) and tumor tissue (TBF). In controls and non-invaded brain regions of tumor-bearing animals, coupling between cerebral perfusion and glucose metabolism was preserved (open circles; $y = 11.2 + 1.7 \star x$, $r = 0.830$, $p < 0.05$). In tumor tissue (closed circles), a TMRglc threshold value of 45.2 ± 15.1 μmol/100 g/min (estimate ± standard error of the estimate) was determined below which local TMRglc declined in parallel with TBF at a slope of 2.0 ml/μmol whereas above 45.2 μmol/100 g/min local TBF did not vary with changes in the glycolytic activity of tumor tissue.

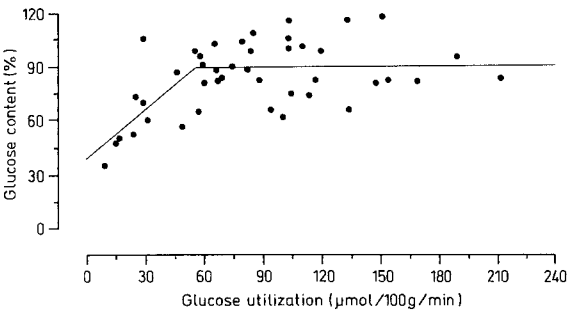

Fig. 5. Relationship between tumor glucose consumption (TMRglc) and glucose content (% optical density of contralateral hemisphere). A TMRglc threshold value of 55 ± 0.2 μmol/100 g/min (estimate ± standard error of the estimate) was estimated for the beginning of the decline of tumor glucose content. In the case of a glucose-dependent increase of the numeric value of the lumped constant, TMRglc values below 55 μmol/100 g/min represent the upper limit of metabolic rates for glucose in these tumor areas.

tumor ATP did not depend on local TBF (Fig. 2, open circles).

The threshold of TBF for the onset of the decline in tumor glucose amounted to 69.0 ± 7.1 ml/100 g/min (Fig. 3). This threshold applied to all five animals and was similar to the TBF/ATP relationship.

– Local relationship of blood flow and glucose utilization

CMRglc and CBF values measured in brain regions of control rats and in non-invaded brain tissue of tumor-bearing animals exhibited a significant linear relationship as determined by regression and correlation analysis (Fig. 4, open circles). This suggests that the coupling between flow and metabolism was preserved. Piecewise linear regression analysis of TBF and TMRglc values, however, revealed a breakpoint parameter value of 45.2 ± 15.1 μmol/100 g/min. Above this value, an increase in local TMRglc was not accompanied by a rise in tumor perfusion (Fig. 4, closed circles). Interestingly, the blood flow/glucose utilization gradients calculated for non-invaded brain regions and for tumor tissue (see Fig. 4) at TMRglc values below 45.2 ± 15.1 μmol/100 g/min were almost identical.

– Local relationship between tumor glucose content and TMRglc

Piecewise linear regression revealed a TMRglc threshold value of 55.0 ± 0.152 μmol/100 g/min for the beginning of the decline in tumor glucose content. As shown in Fig. 5, high rates of tumor glucose utilization were not related to critically low glucose levels in tumor tissue. However, TMRglc values of less than 55.0 μmol/100 g/min may be overestimates because the parallel decline could be associated with an increase in the numerical value of the lumped constant.

– Local relationship between TMRglc and tumor ATP content

The dependency between ATP and local tumor glucose utilization is illustrated in Fig. 6. In the four animals with the highest ATP values, the TMRglc breakpoint was 34.7 ± 4.7 μmol/100 g/min (Fig. 6, closed circles). In the low ATP animal, TMRglc values ranged between 94 to 211 μmol/100 g/min (Fig. 6, open circles). In this tumor, the local energy state declined with increased tumor glycolysis.

– Local relationship between TMRglc and CPS

In Fig. 7, local TMRglc is plotted against protein synthesis expressed in percentages of values for the opposite cortex. A TMRglc threshold for the de-

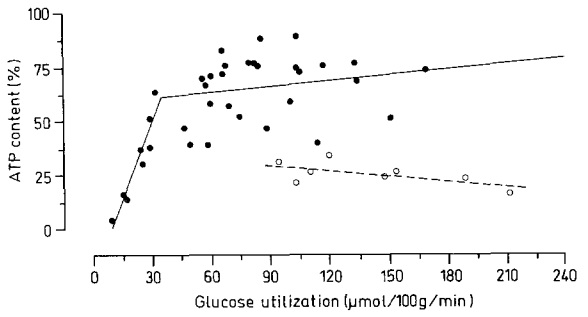

Fig. 6. Relationship between tumor glucose utilization (TMR glc) and ATP content (% optical density of contralateral hemisphere). In one tumor rat revealing the lowest tumor ATP content (21.8 ± 10.4% cf. opposite hemisphere) of the animals studied, the local tumor energy state remained severely suppressed despite TMRglc values varying from 91 to 210 µmol/100 g/min (open circles; $y = 37.2 + 0.09 \star x$). In four out of five animals (closed circles), piecewise linear regression analysis yielded a TMRglc value of 34.7 ± 4.7 µmol/100 g/min (estimate ± standard error of the estimate) for the threshold at which impairment of local tumor energy state begins.

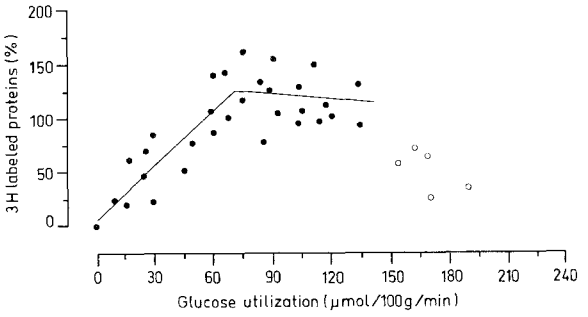

Fig. 7. Relationship between tumor glucose consumption (TMRglc) and amino acid incorporation into tumor proteins (% optical density of labeled proteins in the contralateral cortex). When piecewise linear regression analysis is applied to percentage labeled tumor proteins and corresponding TMRglc values ranging from 0 to 150 µmol/100 g/min (closed circles), a TMRglc threshold of 70.6 ± 8.3 µmol/100 g/min (estimate ± standard error of the estimate) is obtained for the onset of impaired tumor protein synthesis.

cline of protein synthesis was 70.6 ± 8.3 µmol/100 g/min. However, as shown in Fig. 7, protein synthesis also tended to decline with increasing glycolytic activity.

Discussion

One of the most distinctive metabolic particularities which distinguish neoplastic from normal tissue is the tendency for energy-rich metabolites to be generated mostly by glycolysis and less by oxidative phosphorylation [21–26]. Addition of glucose to tumor cell suspensions stimulates glycolysis at the expense of oxidative respiration (Crabtree effect) for the maintenance of stable ATP content [27–29]. Several factors have been proposed to explain this phenomenon, e.g. the pH sensitivity of endogenous respiration, a restriction of the availability of inorganic phosphate or ADP, and an imbalance of the NAD^+/NADH equilibrium (for references [30]). The low oxygen consumption renders tumors relatively insensitive to hypoxia. In human brain tumors submitted to anaerobic conditions, several hours passed before ATP was depleted [31–33].

With the advent of multitracer autoradiography in experimental animals and positron emission tomography (PET) in humans, the effect of brain tumors on local perfusion and metabolism of the non-invaded central nervous system as well as the hemodynamic and metabolic properties of tumors have been investigated in vivo. Although only two control animals were used subjected to the same measurements, the effects of intracerebral tumors on perfusion and glucose metabolism of adjacent and remote brain structures seen in this study corroborate earlier findings observed in experimentally-induced brain tumors [34–39] and in human brain tumors [40, 41]. Remote hemodynamic and matabolic suppression seems to reflect the consequence of cortical deafferentiation rather than of functional diaschitic depression. Neuronal transmission from and to cortex was most probably impaired by the development and spread of vasogenic brain edema into white matter. In both experimental and clinical studies, tumor blood flow (TBF) correlated with tumor size. In small tumors, TBF did not differ from that of surrounding brain tissue whereas in large tumors it was significantly lower, especially in the center of the tumor mass [34, 36, 40, 42–44]. Tumor metabolic rates for glucose (TMRglc) have been shown to vary irrespective of tumor size: in different regions of the same

tumor, TMRglc may be substantially higher, equal or lower than in normal brain tissue [34, 36, 37, 39]. PET investigations of human brain tumors revealed that most tumors exhibit slightly lower TMRglc values than normal brain tissue with a trend towards higher values in high-grade malignant tumors [40, 41, 43, 45]. The rate of oxygen utilization, on the other hand, was consistently reduced [40, 43, 44]. As a consequence, the ratio of oxygen to glucose utilization which in normal brain is about 5.4 mole O_2 per mole glucose declines to 1.9 in brain tumors [43]. This metabolic situation has been called 'aerobic glycolysis' because the low glucose/oxygen uptake ratio is not caused by reduced oxygen supply as in cerebral ischemia.

In the present investigation the relationship between tumor blood flow and metabolism has been investigated in more detail. It appeared that metabolic changes could be detected at surprisingly high flow thresholds: glucose utilization began to decline at flow values below 80 ml/100 g/min, and ATP and glucose content fell at flow values below 70 ml/100 g/min. The beginning of the decline in glucose utilization was associated with a reduction in protein synthesis which started to decline below values of 70 μmol/100 g/min. There was also a threshold relationship between glucose utilization and glucose and ATP content (% O.D. of opposite hemisphere), glucose and ATP falling below values of 55 and 35 μmol/100 g/min, respectively.

Several conclusions can be drawn from these relationships: 1) blood flow limits the glucose supply to tumor tissue at substantially higher flow rates than in normal brain; 2) the decline in tissue glucose is closely associated with a decrease in glucose utilization rate, and 3) the decline in glucose utilization results in a reduction of protein synthesis before the tumor tissue energy state is impaired. Glucose availability, in consequence, is a major determinant of tumor tissue viability, and even minor restrictions result in metabolic disturbances.

The finding of a flow-dependency of tumor glucose supply is surprising. According to our data, below a flow threshold of 69 ml/100 g/min, tumor glucose utilization correlates linearly with tumor perfusion with a slope of about 0.6 μmol/ml (see Fig. 4). The average plasma glucose content of tumor rats was 5.3 μmol/ml (Table 1). Assuming that the peripheral arterial plasma glucose concentration is equal to mean tumor arterial capillary concentration, glucose extraction amounts to maximally 11%. It is unlikely that glucose transport was restricted at the blood-tumor barrier because PET measurements of brain tumors have established a unidirectional extraction fraction for 3-0-methyl-D-glucose of 21% which is close to that of 17% measured in normal cortex. However, it is conceivable that the permeability of tumor cell membranes is lower than in the normal brain. Keller *et al.* (1981) [46] proposed that the cell membrane could be a possible control point of glucose utilization in cultured cells of neuronal origin. If tumor cells exercised a more severe membrane restriction of glucose metabolism than normal brain, this difference might be exploited therapeutically by reducing glucose availability in order to induce selective metabolic disturbances of the tumor cell (see also below).

Our proposal of a limitation of glucose utilization by glucose content of brain tumors is in full agreement with the classical concept of Warburg (1926) [22] who demonstrated a close relationship between the glycolytic rate of cultured tumor cells and the glucose content of the incubation medium. However, we did not observe a decrease of tissue ATP either with high glucose contents or at high glucose utilization rates. Such a relationship was postulated assuming that stimulation of glycolysis-induced lactic acid production led to lethal intracellular acidosis. The absence of this relationship in the present investigation and in an earlier study of various other tumor cell lines [47] suggests that with increasing glucose content, the glycolytic rate may either levels off or that the tumor cell is able to regulate its intracellular pH irrespective of the amount of lactic acid produced.

There are experimental observations in support of both arguments. In Warburg's experiment, glycolytic rate reached a maximum at a glucose concentration in the incubation medium exceeding 5 μmol/ml. It could also be shown that, irrespective of the glycolytic rate, acidosis of brain tumors is rare as long as tissue ATP content is high [47]. This suggests that the tumor is able to control intracellu-

lar pH as long as the energy state is preserved. The appropriate strategy for inducing energy failure in tumors, therefore, may be a reduction and not an increase of glucose level, as suggested before [48].

The other important finding of our investigation is a high threshold of glucose utilization rate for maintenance of protein synthesis. This rate is much higher than that at which energy failure occurs and it is conceivable that protein synthesis of tumor cells – and hence tumor cell viability – may be challenged at a metabolic rate which is still adequate to maintain a normal energy state. Another example of such a dissociation is the postischemic inhibition of protein synthesis which leads to delayed cell death in the CA1 sector of hippocampus CA1 neurons although the tissue energy state is fully preserved. It would be interesting to find out if a similar metabolic situation can be evoked in brain tumors by transiently reducing glucose availability. Further experiments, therefore, should be carried out to test this hypothesis.

References

1. Lantos PL: Chemical induction of tumors in the central nervous system. In: Thomas DGT and Graham DI (eds) Brain Tumors: Scientific Basis Clinical Investigation and Current Therapy. Butterworths, London, 1980, pp 85–108
2. Copeland DD, Vogel FS, Bigner DD: The induction of intracranial neoplasms by the inoculation of avian sarcoma virus in perinatal and adult rats. J Neuropathol Exp Neurol 34: 340–358, 1975
3. Ushio Y, Chernik NL, Shapiro WR, Posner J: Metastatic tumor of the brain: development of an experimental model. Ann Neurol 2: 20–29, 1977
4. Mennel HD, Ivancovic S: Experimentelle Erzeugung von Tumoren des Nervensystems. In: Grundmann E (ed) Handbuch der allgemeinen Pathologie, Bd IV, Tumoren III, Springer, Berlin, Heidelberg, New York, 1975, pp 33–122
5. Benda PH, Someda K, Messer J, Sweet WH: Morphological and immunochemical studies of rat glial tumors and clonal strains propagated in culture. J Neurosurg 34: 310–323, 1971
6. Hossmann K-A, Mies G, Paschen W, Csiba L, Bodsch W, Rapin JR, Le Poncin-Lafitte M, Takahashi K: Multiparametric imaging of blood flow, and metabolism after middle cerebral artery occlusion in cats. J Cereb Blood Flow Metab 5: 97–107, 1985
7. Sakurada O, Kennedy C, Jehle J, Brown JD, Carbin GL, Sokoloff L: Measurement of local cerebral blood flow with iodo(^{14}C)antipyrine. Am J Physiol 234: H59–H66, 1978
8. Sokoloff L, Reivich M, Kennedy C, Des Rosiers MH, Patlak CS, Pettigrew KD, Sakurada O, Shinohara M: The [^{14}C]deoxyglucose method for the measurement of local cerebral glucose utilization: theory, procedure, and normal values in the conscious and anesthetized albino rat. J Neurochem 28: 299–306, 1977
9. Smith CB, Crane AM, Kadekaro M, Agranoff B, Sokoloff L: Stimulation of protein synthesis and glucose utilization in the hypoglossal nucleus induced by axotomy. J Neurosc 4: 2489–2496, 1984
10. Mies G, Niebuhr I, Hossmann K-A: Simultaneous measurement of blood flow and glucose metabolism by autoradiographic techniques. Stroke 12: 581–588, 1981
11. Mies G, Bodsch W, Paschen W, Hossmann K-A: Triple-tracer autoradiography of cerebral blood flow, glucose utilization, and protein synthesis in rat brain. J Cereb Blood Flow Metab 6: 59–70, 1986
12. Kogure K, Alonso OF: A pictorial representation of endogenous brain ATP by a bioluminescent method. Brain Res 154: 273–284, 1978
13. Paschen W, Niebuhr I, Hossmann K-A: A bioluminescent method for the demonstration of regional glucose distribution in brain slices. J Neurochem 36: 513–517, 1981
14. Paschen W, Hossmann K-A, Kerckhoff W vd: Regional assessment of energy-producing metabolism following prolonged complete ischemia of cat brain. J Cereb Blood Flow Metab 3: 321–329, 1983
15. Neter J, Wassermann W, Kutner MH: Applied linear statistical models. Homewood, Illinois, Richard D. Irwin, Inc. 1985
16. Goochee C, Rasband W, Sokoloff L: Computerized densitometry and color coding of ^{14}C-deoxyglucose autoradiographs. Ann Neurol 7: 359–370, 1980
17. Paschen W, Mies G, Kloiber O, Hossmann K-A: Regional quantitative determination of lactate in brain sections. J Cereb Blood Flow Metab 5: 465–468, 1985
18. Sachs L: Angewandte Statistik: Anwendung statistischer Methoden. Berlin, Springer-Verlag, 1984
19. Hürter T, Mennel HD: Experimental brain tumors and edema in rats. I. Histology and cytology of tumors. Acta Neuropathol 55: 105–111, 1981
20. Mennel HD: Transplantation of tumours of the central nervous system induced by resorptive carcinogens. 1. Histological investigation of transplanted tumours of the central nervous system. Neurosurg Rev 1: 123–313, 1978
21. Dickens F, Simer F: Metabolism of normal and brain tumor tissue: II. The respiratory quotient and the relationship of respiration to glycolysis. Biochem J 24: 1031–1326, 1930
22. Warburg O: Über den Stoffwechsel von Tumoren. Springer, Berlin, 1926
23. Warburg O: Metabolism of tumours. London: Constable & Co., 1930
24. Victor J, Wolf A: Metabolism of brain tumors. In: Zabriskie EG, Frantz AN, Hare CC (eds) Tumours of the central

nervous system. An Investigation of the most recent advances. Proc Res Nerv Ment Dis 16: 44–58, 1937.
25. Heller IH, Elliott KAC: The metabolism of normal brain and human gliomas in relation to cell type and density. Canad J Biochem Physiol 33: 395–403, 1955
26. Mahaley MS: The in vitro respiration of normal brain and brain tumors. Cancer Res 26: 195–197, 1966
27. Kvamme E: Glycolysis and respiration in Ehrlich ascites tumor cells. I. Phosphate metabolism in relation to glycolysis and the Crabtree effect. Acta Physiol Scand 42: 204–218, 1958
28. Ibsen KH, Coe EL, McKee RW: Energy compensation in the Crabtree effect with Ehrlich ascites cancer cells. Nature (Lond.) 183: 1471, 1959
29. Quastel JH, Bickis IJ: Metabolism of normal and neoplasms in vitro. Nature (Lond.) 183: 281–289, 1959
30. Ibsen KH: The Crabtree effect: a review. Cancer Res 21: 829–841, 1961
31. Kirsch WM: Substrates of glycolysis in intracranial tumors and analogous normal tissue. Neurology 9: 432–439, 1959
32. Kirsch WM: Substrates of glycolysis in intracranial tumors during complete ischemia. Cancer Res 25: 432–439, 1965
33. Kirsch WM, Schulz D, Leitner JN: The effect of prolonged ischemia upon regional energy reserves in the experimental glioblastoma. Cancer Res 27: 2212–2220, 1967
34. Hossmann K-A, Niebuhr I, Tamura M: Local cerebral blood flow and glucose consumption of rats with experimental gliomas. J Cereb Blood Flow Metab 2: 25–32, 1982
35. Yamada K, Hayakawa T, Ushio Y, Arita N, Kato A, Mogami H: Regional blood flow and capillary permeability in ethyl-nitrosourea induced rat glioma. J Neurosurg 55: 922–928, 1981
36. Yamada K, Ushio Y, Hayakawa T, Arita N, Yamada N, Mogami H: Effects of methylprednisolone on peritumoral brain edema. J Neurosurg 59: 612–619, 1983
37. Blasberg RG, Gazendam J, Shapiro WR, Shinohara WR, Patlak CS, Fenstermacher JD: Clinical implications of quantitative autoradiographic measurements of regional blood flow, capillary permeability and glucose utilization in metastatic brain tumor model. In: Hildebrand J and Gangji D (eds) Treatment of Neoplastic Lesions of the Nervous System. Oxford, Pergamon, 1983, pp 135–141
38. Groothuis D, Blasberg RG, Molnar P, Bigner D, Fenstermacher JD: Regional blood flow in avian sarcoma virus (ASV)-induced brain tumors. Neurology 33: 686–696, 1983
39. Kato A, Diksic M, Yamamoto YL, Feindel W: Quantification of glucose utilization in an experimental brain tumor model by the deoxyglucose model. J Cereb Blood Flow Metab 5: 108–114, 1985
40. Ito M, Lammertsma AA, Wise RJS, Bernardi S, Frackowiak RSJ, Heather JD, McKenzie CG, Thomas DGT, Jones T: Measurement of regional cerebral blood flow and oxygen utilization in patients with cerebral tumours using ^{15}O and positron emission tomography: Analytical techniques and preliminary results. Neuroradiology 23: 63–74, 1982
41. Di Chiro G, DeLaPaz RL, Brooks RA, Sokoloff L, Kornblith PL, Smith BH, Patronas NJ, Kufta CV, Kessler RM, Johnston GS, Manning RG, Wolf AP: Glucose utilization of cerebral gliomas measured by [^{18}F] fluoro-deoxyglucose and positron emission tomography. Neurology 32: 1323–1329, 1982
42. Blasberg RG, Molnar P, Horowitz M, Kornblith R, Pleasants R, Fenstermacher JD: Regional blood flow in RT-9 brain tumors. J Neurosurg 58: 863–873, 1983
43. Rhodes CG, Wise RJS, Gibbs JM, Frackowiak RSJ, Hatazawa J, Palmer AJ, Thomas DGT, Jones T: In vivo disturbance of the oxidative metabolism of glucose in human cerebral gliomas. Ann Neurol 14: 614–626, 1983
44. Leenders KL, Beaney RP, Brooks DJ, Lammertsma AA, Heather JD, McKenzie CG: Dexamethasone treatment of brain tumor patients: effect on regional cerebral blood flow, blood volume and oxygen utilization. Neurology 35: 1610–1616, 1985
45. Herholz K, Ziffling P, Staffen W, Pawlik G, Wagner R, Wienhard K, Heiss W-D: Uncoupling of hexose transport and phosphorylation in human gliomas demonstrated by PET. Eur J Cancer Clin Oncol 24: 1139–1150, 1988
46. Keller K, Lange K, Noske W: D-glucose transport in cultured cells of neuronal origin: the membrane as possible control point of glucose utilization. J Neurochem 36: 1012–1017, 1981
47. Hossmann K-A, Mies G, Paschen W, Szabo L, Dolan E, Wechsler W: Regional metabolism of experimental gliomas. Acta Neuropathol 69: 139–147, 1986
48. von Ardenne M, Reitnauer PG, Rhode K, Westmeyer H: In vivo pH-Messungen in Krebs-Mikrometastasen bei optimierter Übersäuerung. Z Naturforsch 24: 1610–1619, 1969
49. Smith CB, Deibler GE, Eng N, Schmidt K, Sokoloff L: Measurement of local cerebral protein synthesis in vivo: influence of recycling of amino acids derived from protein degradations. Proc Natl Acad Sci 85: 9341–9345, 1988

Address for offprints:
G. Mies,
Max-Planck-Institut für neurologische Forschung,
Abteilung für experimentelle Neurologie,
Ostmerheimer Str. 200,
D-5000 Köln 91, FRG